Available online at www.sciencedirect.com
ScienceDirect
Journal of Photochemistry and Photobiology A: Chemistry 190 (2007) 321–327
Journal of Photochemistry and Photobiology A:Chemistry
www.elsevier.com/locate/jphotochem

Fluorescence resonance energy transfer in dye-labeled DNA

Elena Dolghih, Adrian E. Roitberg, Jeffrey L. Krause *

University of Florida and Department of Chemistry Quantum Theory Project, P.O. Box 118435, Gainesville, FL 32611-8435, United States

Received 6 September 2006; accepted 6 November 2006
Available online 11 November 2006

Abstract

We present the results of molecular modeling of dye-labeled, double-stranded DNA. The structural information obtained from the simulations are used as input to an analysis of energy transfer in this system. The simulations reveal the nature of the interaction between a pair of fluorophores and DNA. The donor, tetramethylrhodamine, TMR, attached to the 5′-end of DNA with a six-carbon tether, interacts primarily with DNA's minor groove, but occasionally stacks against the DNA base pairs. The acceptor, Cy5, attached to the opposite strand at positions n ($n = 7$, 12, 14, 16, 19, 24, 27), binds in the major groove in two distinct locations on the upper and lower part of the groove. We analyzed in detail the dye-to-dye distances, dipole orientation factors and fluorescence resonance energy transfer (FRET) rates. Tests of the validity of the Förster model were conducted using the transition density cube (TDC) method, which provides the exact Coulombic interaction within a certain model chemistry. Our studies show that the use of long tethers does not guarantee rotational freedom of the dyes, as intended in the experiments. Instead, the tethers allow Cy5 to bind in two different geometries, which causes a large uncertainty in the dye-to-dye distances. Our results also show significant fluctuation in the orientation factor, κ^2, which, together with uncertainty in dye-to-dye distances, cause considerable uncertainty in interpreting FRET measurements. We suggest that molecular modeling, combined with the TDC method, provides a useful tool in designing and interpreting FRET experiments.

PACS: 87.10.+e; 87.15.−v

Keywords: DNA; FRET

1. Introduction

Fluorescence resonance energy transfer (FRET) techniques have been in use for several decades [1,2]. However, their application to studies of DNA is fairly recent. One of the first FRET experiments on DNA, performed by Clegg and coworkers in 1993, was a study of the helical geometry of double-stranded DNA (dsDNA) [3]. In 1996, an experiment by Ha et al. demonstrated the possibility of using FRET to study single DNA molecules [4]. A key experiment was conducted in 1999, in which Deniz et al. employed FRET to establish a spectroscopic ruler for measurement of molecular distances in DNA molecules [5]. Since then, the use of FRET in DNA studies has grown rapidly, with applications ranging from investigation of conformational changes of nucleic acids to studies of their dynamics within biological processes [6–8], to applications in nanotechnology [9–11].

FRET techniques are based on measurement of through-space energy transfer between two fluorophores: a donor and an acceptor. The efficiency of this transfer, as defined by Förster theory, depends on the inverse sixth power of the distance R between the two dyes [12],

$$E_{\mathrm{ff}} = \frac{R_0^6}{R^6 + R_0^6}, \tag{1}$$

where R_0 is the Förster radius, the distance at which efficiency is 50%, and R the interchromophore distance. The Förster radius can be defined as:

$$R_0^6 = \frac{9000(\ln 10)\kappa^2 \Phi_{\mathrm{D}}}{128\pi^5 N_{\mathrm{A}} n^4} I, \tag{2}$$

and is related to the rate constant for energy transfer as:

$$k_{\mathrm{RET}} = \frac{1}{\tau_{\mathrm{D}}}\left(\frac{R_0}{R}\right)^6 \tag{3}$$

In these equations, κ^2 is an orientation factor between the donor and acceptor, Φ_{D} the quantum yield of the donor in the absence

* Corresponding author. Tel.: +1 352 392 1597; fax: +1 352 392 8722.
E-mail address: krause@qtp.ufl.edu (J.L. Krause).

1010-6030/$ – see front matter © 2007 Published by Elsevier B.V.
doi:10.1016/j.jphotochem.2006.11.009

of the acceptor, I the spectral overlap of the emission spectrum of the donor with the absorption spectrum of the acceptor (normalized on a wavenumber scale), n the index of refraction of the medium, N_A Avogadro's number, τ_D the lifetime of the donor, and R the distance between the donor and the acceptor. Of the parameters involved in the formulation of Förster theory, the two that introduce the largest uncertainty in FRET measurements are the distance between the dyes and κ^2, the relative orientation of the transition dipoles [1,2].

Notice, in Eq. (2), that all of the quantities required to determine R_0 are either constants, or can be determined via independent experimental measurements. However, R, the distance between the chromophores, cannot be measured directly. As a result, calibration of Förster theory always requires modeling.

The uncertainty in dye-to-dye distance arises from the fact that fluorophores are attached to DNA through tethers, and their location with respect to DNA as well to each other are not defined *a priori*. To investigate this issue, Norman et al. used both FRET and NMR analysis to show that carbocyanine dye, Cy3, when attached to 5′-end of dsDNA, assumes a stacked conformation on top of the molecule. [13] Recently, the positions of TMR and Cy5 with respect to DNA were investigated in several studies. On the basis of fluorescence anisotropy measurements, Dietrich et al. [14], Wang et al. [15] and Unruh et al. [16] concluded that TMR is not a free rotor, and suggested that the dye interacts with DNA. Two molecular dynamics studies confirm this prediction, but differ on the exact nature of the interaction. Dietrich et al. suggest, by analogy with the Texas Red–DNA interaction, that TMR binds to the minor groove [14] while Hillisch et al. report that TMR either interacts with the major groove or stacks on top of DNA [17]. Anisotropy measurements of Cy5 by Dietrich et al. indicate that its dynamics, as with TMR, are coupled to that of DNA [14].

The relative orientation of the dipoles of the donor and acceptor is another source of uncertainty in FRET measurements. The orientation factor, κ^2, can vary from 0 to 4, corresponding to dipoles aligned perpendicular and parallel to each other, respectively. Since it is difficult experimentally to determine the exact value of κ^2, a value of 2/3 is often assumed [18] corresponding to dynamically averaged dipole orientations of rotationally free chromophores. The validity of this assumption has been discussed in several previous studies [19–21] with arguments proposed both for and against this approximation. Recently Wong et al. proved explicitly that energy transfer efficiency does indeed depend on the orientation factor [22]. In a theoretical study, the authors analyzed the dependence of energy transfer rates on κ^2 in a system of dyes with controlled dipole orientations. In addition, Lewis et al. described a systematic study of FRET orientation factors, in which the dependence of the quantum yield and donor lifetime on κ^2 were revealed [23]. Neither study, however, investigated the effects of dynamic fluctuations of the orientation factor or estimated the resultant uncertainty in average κ^2.

In reviewing the extant literature, it is apparent that significant uncertainty exists concerning the positions of the dyes with respect to DNA as well as their relative orientations. In this paper, we investigate this issue by performing molecular dynamics simulations of TMR and Cy5 dyes attached to DNA. In addition to obtaining data that are difficult to determine experimentally, the simulations illustrate how fluctuations in distance and orientation of the dyes affect the interpretation of results via the Förster model. A close analysis of dipole orientation factors, dye-to-dye distances and energy transfer rates enable us to evaluate the accuracy of the assumptions that are often made in FRET DNA experiments. Our results allow us to offer suggestions for improving the design and interpretation of these and related experiments. We also demonstrate clearly the critical role of modeling in determining R, the one parameter in Förster theory than cannot be determined experimentally.

2. Methods

The system studied consisted of the donor–acceptor-labeled, double-stranded DNA considered in the experiments of Deniz et al. [5]. The donor, tetramethylrhodamine (TMR) was attached with a six-carbon tether at 5′-end of DNA strand with the following sequence:

5′-CTCTTCAGTTCACAGTCCATCCTATCAGCCGCTTG-CCTTC-3′.

The acceptor, a carbocyanine dye Cy5, was attached at locations n (n = 7, 12, 14, 16, 19, 24, 27) of the opposite strand. To decrease simulation time, six additional base pairs were included after each Cy5 dye, rather than modeling the full 40 base-pair sequences used in the Deniz et al. experiments. Control runs with a 33 base-pair DNA sequence showed no difference in the results.

Our simulations used the *parm99* force field for DNA and the general amber force field (gaff) for the dyes, as provided by AMBER 9.0 software package [24]. Electrostatic solvent effects were simulated using the generalized Born model [25] which was shown previously to work well for nucleic acids, as compared with explicit solvent simulations, which are much more time-consuming [26]. We used mBondi radii for the atoms and 0.13 Å offset of the effective Born radii. Along with the SHAKE algorithm, Langevin dynamics with a friction coefficient of 10 ps^{-1} were employed, the ionic strength was set at 0.2 M and cutoff at 20.0 Å for the non-bonded interactions. To improve the efficiency of the calculations, nrespa was set to 2 and rgbmax to 20. We followed equilibration procedures similar to those used typically in DNA simulations [26,27]. First, structures were restrained harmonically with a 5 kcal/(mol $Å^2$) force constant and minimized for several cycles, while gradually lowering the restraint to 1 kcal/(mol $Å^2$). Then, the molecules were equilibrated for 60 ps, while increasing the temperature to 300 K. Finally, the production run was initiated at 300 K, without any restraints. The time step was set to 2 fs and results were recorded every 1000 steps. The length of the runs was 20 ns, with longer test runs to assure convergence.

Fluorescence resonance energy transfer is based on a Coulombic interaction between two chromophores. Förster theory approximates this interaction through a dipole–dipole

expansion of the potential,

$$V^{\mathrm{Coul}} \approx V^{\mathrm{dip-dip}} = \frac{1}{4\pi\epsilon_0}\frac{\kappa\mu_{\mathrm{D}}\mu_{\mathrm{A}}}{R^3} \tag{4}$$

where ϵ_0 is vacuum permittivity constant, κ the orientation factor, $\mu_{\mathrm{D,A}}$ the ground to first excited state transition dipole moments of the donor and acceptor, and R the distance between the two dipoles. The transition density cube method provides an alternative representation, in which the Coulombic coupling between the donor and acceptor is calculated based on a sum of transition density cube elements, $M_{\mathrm{D}}^{\mathrm{eg}}(i)$ and $M_{\mathrm{A}}^{\mathrm{eq}}(j)$ [28]. In this method,

$$V^{\mathrm{Coul}} \cong \sum_{i,j}\frac{M_{\mathrm{D}}^{\mathrm{eg}}(i)M_{\mathrm{A}}^{\mathrm{eq}}(j)}{4\pi\epsilon_0 r_{ij}}, \tag{5}$$

where the transition densities are defined as:

$$M_{\mathrm{N}}(\mathbf{r}) = \int_{\mathrm{s}}\Psi_{\mathrm{Ng}}\Psi_{\mathrm{Ne}}^{*}\mathrm{d}s\mathrm{d}\mathbf{r}, \tag{6}$$

for $N = \mathrm{D}, \mathrm{A}$. Note that the integral in Eq. (6) is only over spin. The rate constant is then defined as:

$$k_{\mathrm{RET}} = \frac{1}{\hbar^2 c}|V^{\mathrm{Coul}}|^2 J, \tag{7}$$

where $\hbar$ is Planck's constant in units of cm^{-1} s, V^{Coul} is in cm^{-1}, and J is the spectral overlap of the emission spectrum of the donor with the absorption spectrum of the acceptor normalized on an energy scale. In the limit of small cube size, the TDC method provides an exact representation of the Coulombic interaction (for a given quantum mechanical method and basis set). Calculations of the TDC elements were performed using the Q-Chem software package with the Hartree-Fock method and a 6–31G* basis set. The excited states were determined using Configuration Interaction Singles (CIS) with only singlet excited states computed. The number of cube elements was set to 50,000 with test runs with larger values to assure convergence. A TDC analysis was conducted at every fifth frame of the last 10 ns of each run (1000 frames in total). Förster radii and energy transfer rates were calculated for each frame and then averaged for each run.

The following values for the Förster radii calculations for the TMR–Cy5–DNA system were used: $I = 9.9 \times 10^{-13}\ \mathrm{cm}^3/\mathrm{M}$ [29], $n = 1.33$ [29] and $\Phi_{\mathrm{D}} = 0.56$ [30]. For TDC rate calculations, the spectral overlap was determined from experimental spectra $J = 1.26 \times 10^{-4}$ cm [15,31]. Note that the two overlap values are different due to different normalization unit scales.

3. Results and discussion

In FRET studies involving DNA, the dye-to-dye distances can be estimated using a theoretical model introduced by Clegg et al. [3]. Within this model, the interdye distance is calculated using the following formula [14]:

$$R = ((L + 3.4\Delta N)^2 + (a^2 + d^2 - 2ad\ \cos(\theta + 36\Delta N))^{1/2}, \tag{8}$$

where L is the separation in distance between the two dyes along the helical axes for zero base pairs, ΔN the base pair separation, θ the angular separation between the dyes for zero base pairs, and d and a are the normal distances of the donor and acceptor to the DNA helical axes, respectively. While the Clegg model is known to provide a highly accurate description of the classic B-DNA structure, the distances a and d of the fluorophores from the DNA axis are unknown. Their estimates, supported at best by fluorescence anisotropy studies, vary from 15 Å, corresponding to both dyes fully extended away from DNA [5,14] to 0 Å, implying close interaction with the DNA molecule [14,30]. Results of our simulations indicate that the dynamics of both TMR and Cy5 are coupled to the dynamics of the DNA host. TMR is found to bind in the minor groove of DNA, occasionally assuming a stacked conformation on top of the molecule, while Cy5 is observed to bind in two primary locations in the major groove, an upper position, and a lower position (see Fig. 1). These findings confirm previous reports of high anisotropy values for both fluorophores [14–16]. They also support, in part, the molecular dynamics results of Unruh et al. involving TMR [16]. The tendency of TMR to assume two slightly different positions with respect to DNA agrees with experimental reports of at least two lifetimes for this dye [32,33]. The flexibility of the six-atom linker appears to allow Cy5 to bind in two different locations in the major groove, resulting in an average interdye distance difference of 8 Å between the two conformers. Both TMR and Cy5 fluctuate between their different positions within the nanosecond timescale of the simulation, without a noticeable change in the total potential energy of the system. Although the simulations probably greatly underestimate the transition time, these results suggest that the different conformations of Cy5 occur with nearly equal frequency on the timescale of the experimental measurements (milliseconds). The observed single-peak distributions of experimental efficiencies, rather then multiple peaks, suggest the same conclusion.

The interdye distances were measured between the centers of the dyes throughout the molecular dynamics simulations. The values were then averaged for each dye–DNA construct with an assumption that both Cy5 conformations occur with the equal frequency (see Table 1). For comparison, we provide distance values predicted by the Clegg model for fully extended dyes (assuming that a and d equal 15 Å), as well as for dyes interacting closely with the DNA (a and d equal 0 Å). As can be seen in

Table 1
Interchromophore distances as calculated with the Clegg model compared to distances obtained from the simulations

N_{bp}	Clegg Model ($d = a = 15$ Å)	Clegg Model ($d = a = 0$ Å)	MD
7	38.5	28.8	20.7 ± 1.4
12	48.4	45.8	46.1 ± 3.5
14	52.6	52.6	48.9 ± 8.8
16	62.5	59.4	49.6 ± 5.3
19	75.7	69.6	68.8 ± 4.8
24	86.6	86.6	82.1 ± 4.1
27	100.1	96.8	88.9 ± 6.7

All distances are in Å.

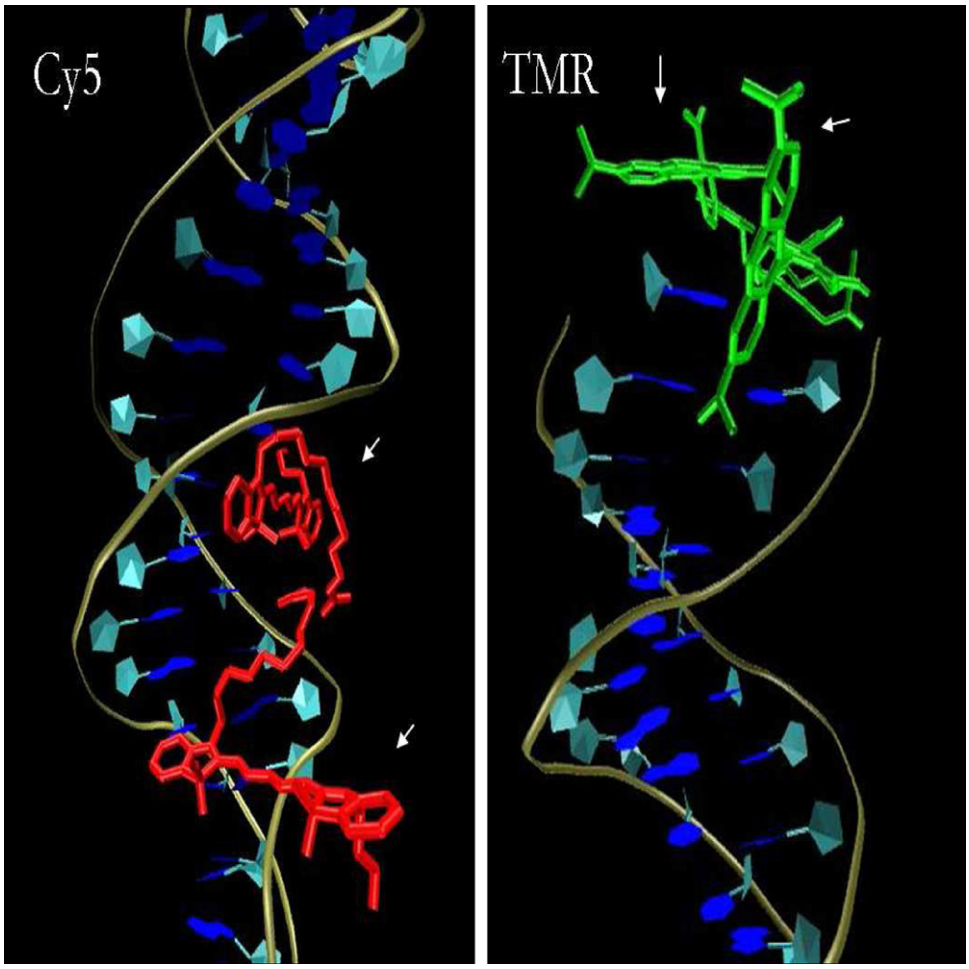

Fig. 1. Dye conformations in DNA. The acceptor, Cy5 (left panel) interacts with major groove of DNA in two main conformations, an upper configuration and a lower configuration (marked with arrows). The donor, TMR (right panel) interacts with the minor groove of DNA or in a stacked configuration (marked with arrows).

the table, the distances obtained from the simulations, while in general smaller then those predicted by either of the theoretical models, fit more closely to the second model, with an average uncertainty of about 5 Å. Although this difference is not large, the standard deviation of the average values in some cases is as high as 8 Å. Large fluctuations in the distance arise from the presence of multiple conformations of Cy5. This phenomenon both complicates the distance analysis and introduces a large uncertainty in the distances obtained by Förster analysis.

In conventional applications of the Förster formula, the orientation factor, κ^2, is often set equal to 2/3, on the assumption that the dyes are rotating freely and all dipole orientations are sampled equally. Experimentally, however, there is no guarantee that this is the case. As our simulations show, both TMR and Cy5 are coupled to DNA in their motion, which results in limited rotational freedom. This hindered motion of the dyes does not have a dramatic effect on the average κ^2 values (calculated for each frame and then averaged for each run). We find that in most cases $\langle\kappa^2\rangle$ lie within 45% of 0.67. While this is might be an acceptable range of variation, as Fig. 2 shows, similar average values of the orientation factor can correspond to very different distributions. In this figure, the two distributions (1000 frames each) are obtained from MD simulations corre-

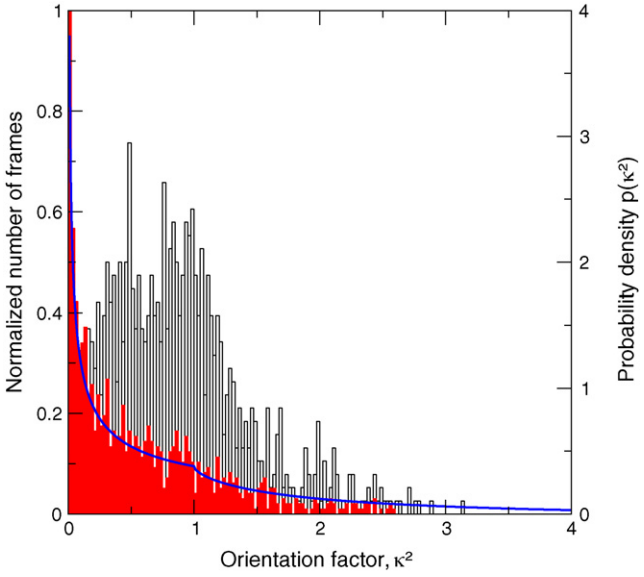

Fig. 2. Dipole orientations factors, κ^2. Distributions are shown for two simulations, one with an average κ^2 of 0.84 (open bars), and the other with an average κ^2 of 0.86 (solid bars). The solid line represents the theoretical prediction for the $P(\kappa^2)$ expected for $\langle\kappa^2\rangle = 2/3$.

Table 2
Effect of κ^2 on calculated efficiencies, as described in the text

$\langle\kappa^2\rangle$	Efficiency
0.86	0.65 ± 0.29
0.84	0.56 ± 0.29
0.86	0.84

sponding to $n = 12$ and $n = 16$ DNA constructs. The average κ^2 in one case is 0.84, and the other is 0.86. Also shown in the figure is the theoretical distribution derived from the $P(\kappa^2)$ that gives $\langle\kappa^2\rangle = 2/3$ [34]. Notice, in this case, that the distribution corresponding to $\langle\kappa^2\rangle = 0.86$ matches the theoretical distribution for $\langle\kappa^2\rangle = 2/3$ rather closely, while the distribution for $\langle\kappa^2\rangle = 0.84$ is completely different. Moreover, as shown in Table 2, the two distributions result in different average efficiency values when calculated using the Förster formula. Here, even though R is slightly different for the two constructs, we used a single value in both calculations (an average of one of the runs) so that any observed fluctuation in the efficiencies reflect only variation in the orientation factor. Thus, the first two rows of the table reflect average efficiencies corresponding to the two different distributions of κ^2 in Fig. 2. The two values were calculated via the following formula:

$$E_{\mathrm{ff}} = \left\langle \frac{R_0^6}{R_0^6 + \langle R\rangle^6} \right\rangle, \tag{9}$$

where $\langle R\rangle = 54.4$ Å and R_0 was calculated independently for each frame. In the third row of the table, the efficiency was calculated as in Eq. (1), using an average value of R_0 based on $\langle\kappa^2\rangle = 0.86$ and the same average value of R as above. As one can see in the table, using $\langle\kappa^2\rangle$ can result in very different efficiencies than those obtained using the true distribution of κ^2.

Using the Förster formula, we calculated average efficiencies for each oligonucleotide, assuming that both conformations of Cy5 are equally probable. As shown in Fig. 3, the calculated efficiencies are very close to the mean experimental efficiencies reported by Deniz et al. [5], when plotted versus the values of R determined from the simulations. The agreement deteriorates when the experimental data are plotted versus the distances obtained using the Clegg model. This confirms our prediction that Cy5 exists in two conformations under experimental conditions. Even more interesting is that neither our calculations, nor the experimental measurements fit the R^{-6} dependence predicted by Förster (see Fig. 4). Shown in the figure are four lines. One plots the experimental data, using the values of R obtained from the Clegg model. This line has a slope of 4.3. A second line plots the results of the simulations, with the Cy5 fixed in one of its conformations, and the values of R determined theoretically, with an average R_0 determined from the simulation This line has a slope of 6.0, as it must, since the efficiencies are determined using the Förster formula (Eq. (1)). A third line shows the experimental efficiencies versus the theoretical values of R, with a slope of 3.7. The fourth line shows average theoretical efficiencies assuming that the Cy5 adopts two conformations (and that each conformation obeys the Förster scaling), as calculated with

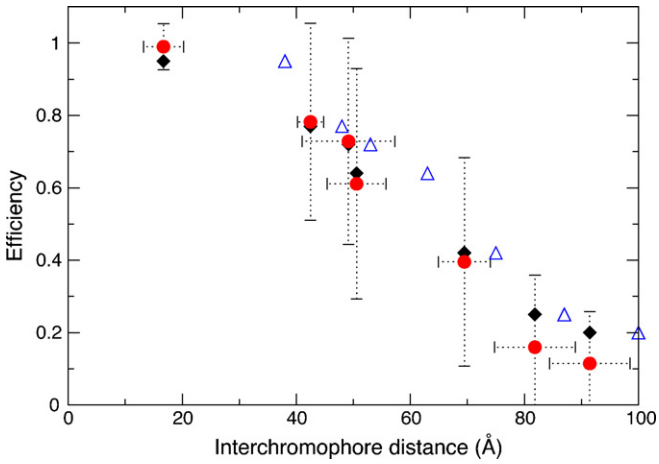

Fig. 3. Förster efficiencies, theory vs. experiment. The experimental data of Deniz et al. [5] are shown as solid diamonds and open triangles, and the theory is shown as solid circles. The experimental data are plotted vs. the distances obtained using the Clegg model (triangles) and vs. the distances obtained from the simulations (diamonds).

the following formula:

$$\langle E_{\mathrm{ff}}\rangle = \frac{1}{2}\left(\frac{1}{1+(R/R_0)^6} + \frac{1}{1+(R+\alpha/R_0+\beta)^6}\right). \tag{10}$$

In this formula, $\alpha = 7.79$ Å is the average difference in distance between the two conformations of Cy5 and TMR, and $\beta = 13.53$ Å is the average difference in the Förster radius for the two conformations. The slope of this line is 5.0. While we are not suggesting that this is the correct method to calculate the efficiencies (one would need to do an ensemble average over all conformations adopted by both dyes), Fig. 4 illustrates clearly that adding a single additional configuration results in a weaker R dependence than the Förster prediction of R^{-6}. Our conjecture is that including all relevant configurations in the average

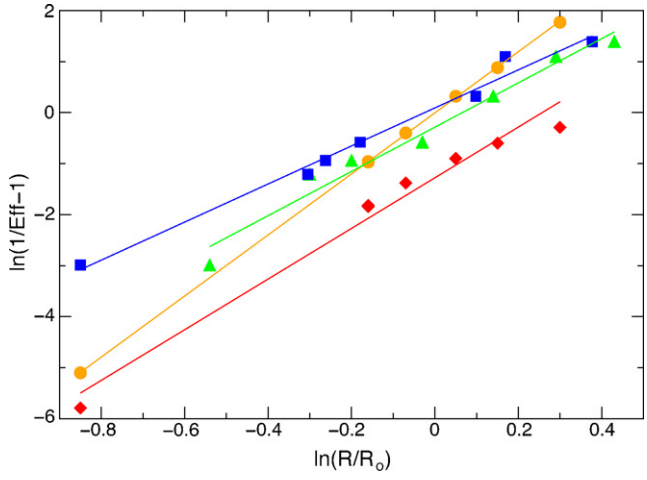

Fig. 4. Effects of multiple fluorophore conformations. The experimental data of Deniz et al. [5] are shown an solid triangles, the experimental data with the theoretical distances are plotted as solid squares, the theoretical data for a single configuration are plotted as solid circles, and the theoretical data for two configurations (as discussed in the text) are plotted as solid diamonds. The slopes are, respectively, 4.3, 3.7, 6.0 and 5.0.

Table 3
FRET rate constants calculated using Förster theory and the TDC, for varying numbers of base pairs between the chromophores

N_{bp}	k_{TDC} (ns^{-1})	$k_{Förster}$ (ns^{-1})
7	54.0	143
12	1.54	4.18
14	2.11	5.34
16	0.72	2.08
19	0.12	0.36
24	0.07	0.20
27	0.03	0.08

would bring the theoretical predictions in better agreement with experiment.

In addition to calculating interdye distances and orientation factors, the TDC method can be used to calculate rates of energy transfer. In Table 3, we compare TDC rates to those calculated with the dipole–dipole approximation of Förster theory. As expected, when the interdye distance becomes comparable to the size of the dyes ($n \sim 7$), the Förster model overestimates the rate. This would be of significant concern in future work on systems in which the distance between the dyes is relatively short. An additional potential advantage to employing TDC is the ability to predict efficiencies using TDC rate constants and the following equation:

$$E_{ff} = \frac{k_{TDC}}{k_{TDC} + \tau^{-1}}, \tag{11}$$

where τ^{-1} is the donor lifetime. This method eliminates the Förster imposed R^{-6} dependence completely. Unfortunately, in the Cy5–DNA–TMR system, TMR is known to have several lifetimes [32,33]. This, in addition to contributing to the uncertainty in experimental measurements, results in poor prediction of efficiencies using Eq. (11). However, for systems in which the lifetime is better defined, this approach provides an additional test of the Förster model. In fact, as this work shows, the TDC method can be of essential help in providing the input to the design and testing of experimental systems, as well in interpreting FRET results.

4. Conclusions

While FRET experiments are often performed on dye-labeled DNA, the position of the dyes with respect to DNA and their relative orientation are seldom well-defined, which precludes an accurate application of Förster theory. Our study of a dye-labeled DNA model shows that TMR and Cy5, two dyes commonly used in FRET experiments, interact with DNA and assume multiple conformations that interconvert on the time-scale of the experiment. Analysis with the transition density cube method reveals that this behavior causes large fluctuations in both the interchromophore distance and the orientation factor, which results in a broad distribution of experimental efficiencies. Moreover, the presence of at least two conformations of Cy5 causes a breakdown of the Förster-predicted R^{-6} scaling. Based on our results, it is apparent that quantitative predictions of Förster theory require detailed knowledge of the dye–DNA system under investigation. Another possibility is to use a system with an intrinsic, rigid control of the position and orientation of the dyes. One such system could involve dyes that assume stacked conformations on the ends of the DNA [23]. Another approach might involve fluorescent analogs of DNA nucleotides serving as either donors, acceptors or both [35]. Finally, one possible method to improve the system discussed in this work would be to shorten the tethers linking the dyes to the DNA. This might lead to less interaction of the dyes with the helix. Theoretical investigation of this idea is underway.

Acknowledgments

This work was partially supported by the Department of Energy through grant DE-FG02-02ER45995. Supercomputing time at NCSA through allocation MCA05S010 to AER is acknowledged gratefully.

References

[1] S. Weiss, Fluorescence spectroscopy of single biomolecules, Science 283 (1999) 1676–1683.
[2] P.R. Selvin, The renaissance of fluorescence resonance energy transfer, Nat. Struct. Biol. 7 (2000) 730–734.
[3] R.M. Clegg, A.I.H. Murchie, A. Zechel, D.M.J. Lilley, Observing the helical geometry of double-stranded DNA in solution by fluorescence resonance energy transfer, Proc. Nat. Acad. Sci. USA 90 (1993) 2994–2998.
[4] T. Ha, T. Enderle, D.F. Ogletree, D.S. Chemla, P.R. Selvin, S. Weiss, Probing the interaction between two single molecules: fluorescence resonance energy transfer between a single donor and a single acceptor, Proc. Natl. Acad. Sci. USA 93 (1996) 6264–6268.
[5] A.A. Deniz, M. Dahan, J.R. Grunwell, T. Ha, A.E. Faulhaber, D.S. Chemla, S. Weiss, P.G. Schultz, Single-pair fluorescence resonance energy transfer on freely diffusing molecules: observation of förster distance dependence and subpopulations, Proc. Natl. Acad. Sci. USA 96 (1999) 3670–3675.
[6] J.R. Grunwell, J.L. Glass, T.D. Lacoste, A.A. Deniz, D.S. Chemla, P.G. Schultz, Monitoring the conformational fluctuations of DNA hairpins using single-pair fluorescence resonance energy transfer, J. Am. Chem. Soc. 123 (2001) 4295–4303.
[7] M.C. Murphy, I. Resnik, W. Cheng, T.M. Lohman, T. Ha, Probing single-stranded DNA conformational flexibility using fluorescence spectroscopy, Biophys. J. 86 (2004) 2530–2537.
[8] M. Karymov, D. Daniel, O.F. Sankey, Y.L. Lyubchenko, Holliday junction dynamics and branch migration: single-molecule analysis, Proc. Natl. Acad. Sci. 102 (2005) 8186–8191.
[9] V. Viasnoff, A. Meller, H. Isambert, DNA nanomechanical switches under folding kinetics control, Nanoletters 6 (2006) 101–104.
[10] M. Heilemann, P. Tinnefeld, G.S. Mosteiro, M.G. Parajo, N.F. van Hulst, M. Sauer, Multistep energy transfer in single molecular photonic wires, J. Am. Chem. Soc. 126 (2004) 6514–6515.
[11] S. Vyawahare, S. Eyal, K.D. Mathews, S.R. Quake, Nanometer-scale fluorescence resonance optical waveguides, Nanoletters 4 (2004) 1035–1039.
[12] T. Förster, Intermolecular energy migration and fluorescence, Ann. Physik. 2 (1948) 55–75, translated by R.S. Knox, Department of Physics and Astronomy, University of Rochester, Rochester, NY 14627.
[13] D.G. Norman, R.J. Grainger, D. Uhrïn, D.M. Lilley, Location of cyanine-3 on double-stranded DNA: importance for fluorescence resonance energy transfer studies, Biochemistry 39 (2000) 6317–6324.
[14] A. Dietrich, V. Buschmann, C. Müller, M. Sauer, Fluorescence resonance energy transfer (fret) and competing processes in donor-acceptor substituted DNA strands: a comparative study of ensemble and single-molecule data, Rev. Mol. Biotechnol. 82 (2002) 211–231.
[15] L. Wang, A.K. Gaigalas, J. Blasic, M.J. Holden, Spectroscopic characterization of fluorescein- and tetramethylrhodamine-labeled oligonucleotides

and their complexes with a DNA template, Spectrochim. Acta Part A 60 (2004) 2741–2750.
[16] J.R. Unruh, G. Gokulrangan, G.H. Lushington, C.K. Johnson, G.S. Wilson, Orientational dynamics and dye–DNA interactions in a dye-labeled DNA aptamer, Biophys. J. 88 (2005) 3455–3465.
[17] A. Hillisch, M. Lorenz, S. Diekmann, Recent advances in fret: distance determination in protein–DNA complexes, Curr. Opin. Struct. Biol. 11 (2001) 201–207.
[18] B. van der Meer, Kappa-squared: from nuisance to new sense, Rev. Mol. Biotech. 82 (2002) 181–196.
[19] C.G. dos Remedios, P.D.J. Moens, Fluorescence resonance energy transfer spectroscopy is a reliable "ruler" for measuring structural changes in proteins, J. Struct. Biol. 115 (1995) 175–185.
[20] P. Wu, L. Brand, Orientation factor in steady-state and time-resolved resonance energy transfer measurements, Biochemistry 31 (1992) 7939–7947.
[21] E. Haas, E. Katchalski-Katzir, I.Z. Steinberg, Effect of the orientation of donor and acceptor on the probability of energy transfer involving electronic transitions of mixed polarization, Biochemistry 17 (1978) 5064–5070.
[22] K.F. Wong, B. Bagchi, P.J. Rossky, Distance and orientation dependence of excitation transfer rates in conjugated systems: beyond the förster theory, J. Phys. Chem. A 108 (2004) 5752–5763.
[23] F.D. Lewis, L. Zhang, X. Zuo, Orientation control of fluorescence resonance energy transfer using DNA as a helical scaffold, J. Am. Chem. Soc. 127 (2005) 10002–10003.
[24] D.A. Case, T.A. Darden, T.E. Cheatham III, C.L. Simmerling, J. Wang, R.E. Duke, R. Luo, K.M. Merz, D.A. Pearlman, M. Crowley, R.C. Walker, W. Zhang, B. Wang, S. Hayik, A. Roitberg, G. Seabra, K.F. Wong, F. Paesani, X. Wu, S. Brozell, V. Tsui, H. Gohlke, L. Yang, C. Tan, J. Mongan, V. Hornak, G. Cui, P. Beroza, D.H. Mathews, C. Schafmeister, W.S. Ross, P.A. Kollman, AMBER 9, University of California, San Francisco, 2006.
[25] G.D. Hawkins, C.J. Cramer, D.G. Truhlar, Pairwise solute descreening of solute charges from a dielectric medium, Chem. Phys. Lett. 246 (1995) 122–129.
[26] V. Tsui, D.A. Case, Molecular dynamics simulations of nucleic acids with a generalized born solvation model, J. Am. Chem. Soc. 122 (2000) 2489–2498.
[27] G. Cui, C. Simmerling, Conformational heterogeneity observed in simulations of a pyrene-substituted DNA, J. Am. Chem. Soc. 124 (2002) 12154–12164.
[28] B.P. Krueger, G.D. Scholes, G.R. Fleming, Calculation of couplings and energy-transfer pathways between the pigments of lh2 by the ab initio transition density cube method, J. Phys. Chem. B 102 (1998) 5378–5386.
[29] B. Zimmerman, M. Diez, N. Zarrabi, P. Gräber, M. Börsch, Movement of the ε-subunit during catalysis and activation in single membrane-bound h^+-atp, Eur. Mol. Biol. Org. 24 (2005) 2053–2063.
[30] N.K. Lee, A.N. Kapanidis, Y. Wang, X. Michalet, J. Mukhopadhyay, R.H. Ebright, S. Weiss, Accurate fret measurements within single diffusing biomolecules using alternating-laser excitation, Biophys. J. 88 (2005) 2939–2953.
[31] U. Schobel, H.-J. Egelhaaf, A. Brecht, D. Oelkrug, G. Gauglitz, New donor–acceptor pair for fluorescent immunoassays by energy transfer, Bioconjug. Chem. 10 (1999) 1107–1114.
[32] L. Edman, Ü. Mets, R. Rigler, Conformational transitions monitored for single molecules in solution, Proc. Natl. Acad. Sci. USA 93 (1996) 6710–6715.
[33] H. Kojima, N. Spataru, Y. Kawata, S. Yano, I. Vartires, Long-ranged electron interaction between carboxytetramethylrhodamine and fluoresceinisothiocyanate bound covalently to DNA, as evidenced by fluorescence quenching, J. Phys. Chem. B 102 (1998) 9981–9984.
[34] B.W. der Meer, G. Coker, S.-Y. Chen, Resonance Energy Transfer: Theory and Data, VCH Publishers Inc., New York, 1994.
[35] J.M. Jean, K.B. Hall, 2-Aminopurine fluorescence quenching and lifetimes: role of base stacking, Proc. Natl. Acad. Sci. 98 (2001) 37–41.